Planar Array of Electric-LC Resonators With Broadband Tunability

Withawat Withayachumnankul, *Member, IEEE*, Christophe Fumeaux, *Senior Member, IEEE*, and Derek Abbott, *Fellow, IEEE*

***Abstract*—A planar array of microwave electric-LC (ELC) resonators with broadband tunability of the resonance frequency is presented in this letter. An ELC resonator is typically composed of inductive loops and a capacitive gap, resonant at a wavelength much larger than its physical dimension. Here, the original resonator is modified to accommodate a varactor and its accompanying dc bias enabling resonance tunability. The wideband operation can be achieved through strategic placement of the varactor. The robustness of the response for a large array containing hundreds of the varactor-loaded resonators is considered via a sensitivity analysis. The numerical and experimental results show that the fabricated array possesses a wide tuning range of nearly 32% with no significant resonance broadening, despite the tolerance in varactor characteristics.**

***Index Terms*—Electric LC (ELC) resonator, frequency selective surface, metamaterial, tunability.**

I. Introduction

THE ELECTRIC-LC (ELC) resonator was proposed as a building block in metamaterials, providing customizable values of the permittivity [1]–[3]. A single ELC resonator comprises symmetric metallic loops and dielectric gaps, forming an equivalent LC circuit, whose resonance frequency is predominantly governed by the shape and dimensions of the resonator. Owing to their unusual properties, ELC resonators have been realized for many types of devices, e.g., absorbers [4], [5], reflectors [6], modulators [7], polarizers [8], [9], and wave plates [10].

Many ELC resonators with a frequency-tuning capability have been proposed in the microwave [11] and terahertz regimes [12]–[14]. This flexibility allows realization of advanced applications. For the microwave ELC resonators proposed in [11], it is suggested that a ferrite element be introduced in the unit cell to enable tuning of the resonance frequency. However, an external static magnetic field is required to manipulate the permeability of ferrite, whose nonlinearity and anisotropy greatly complicate the analysis and implementation. These issues can be overcome with an electrical-control approach, as implemented with split-ring resonators [15] and in a reflectarray of complementary ELC resonators [16].

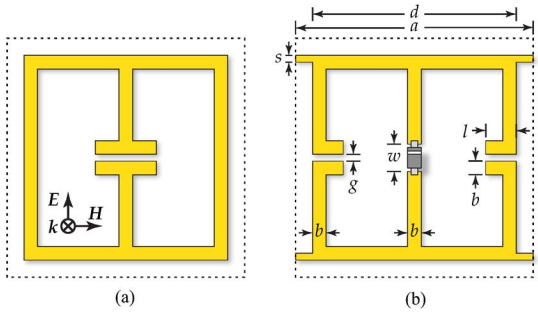

Fig. 1. ELC resonators. (a) Original ELC resonator. (b) ELC resonator with a varactor loaded at the central gap. The dc bias is positioned at the four corners of the loaded resonator. The dotted lines bound each unit cell.

Accordingly, we propose a design of microwave ELC resonators that are loaded with varactors to sweep the resonance frequency. In this approach, two important problems are now addressed: 1) wideband tunability, and 2) resonance broadening for a large resonator array. By loading a varactor at a particular location on the resonator, wideband tunability can be achieved. The proposed concept is validated through simulation and experiment in the transmission mode. A sensitivity analysis is carried out to ensure the robustness of the fabricated array. These two aspects extend the functionality of the ELC resonator beyond its original application in metamaterials toward a more general use in advanced microwave devices.

II. Design

An original ELC resonator [1] is shown in Fig. 1(a). In the quasistatic limit, the resonator can be approximated by the inductor and capacitor in the form of an LC resonant circuit. Specifically, the central gap forms the capacitor, while the conducting loops form the inductors. In normal operation, an oscillating electric field polarized perpendicularly to the gap induces a current flow in the two symmetric loops. Similar to an electronic LC circuit, the structure becomes resonant when the electric energy stored in the capacitor is equal to the magnetic energy stored in the inductor.

The resonance frequency can be tuned by altering the capacitance or inductance in the structure [17]. For operation at microwave frequencies, a variable capacitor or varactor can be incorporated into the original ELC resonator. Essentially, a varactor exploits the depletion region in the p-n junction of a diode for its operation. For a large dc reverse bias, the depletion region expands, and hence the junction capacitance decreases. Vice

Manuscript received April 10, 2011; revised May 23, 2011; accepted May 28, 2011. Date of publication June 07, 2011; date of current version June 23, 2011. This was supported by the Australian Research Council Discovery Projects funding scheme under Project DP1095151.

W. Withayachumnankul is with the School of Electrical and Electronic Engineering, The University of Adelaide, Adelaide, SA 5005, Australia, and also with the School of Electronic Engineering, Faculty of Engineering, King Mongkut's Institute of Technology Ladkrabang, Bangkok 10520, Thailand (e-mail: withawat@eleceng.adelaide.edu.au).

C. Fumeaux and D. Abbott are with the School of Electrical & Electronic Engineering, The University of Adelaide, Adelaide, SA 5005, Australia.

Color versions of one or more of the figures in this letter are available online at http://ieeexplore.ieee.org.

Digital Object Identifier 10.1109/LAWP.2011.2158794

versa, for a small reverse bias, the capacitance increases as a result of a thinner depletion region. In principle, it is possible to load a tuning varactor at any location on the conducting strip, provided that the resonator remains symmetric and the two varactor ports are dc-isolated. However, this does not yield optimal tunability for the ELC resonator.

The optimum tunability can be achieved by placing a varactor at the location where the voltage gradient or the absolute current, induced by an incident wave, is maximum [18]. For the ELC resonator, this maximum voltage gradient occurs in the middle of the central strip. By considering that a varactor requires dc isolation between its two ports, the varactor-loaded ELC resonator now evolves into the form in Fig. 1(b). This design is similar to a variant of ELC resonators [2] and a nonlinear electric metamaterial [19]. The two gaps on both sides couple to the incident electric field and, at the same time, provide an electrical isolation to the varactor ports.

Also shown in Fig. 1(b), there are extra conductor strips at the corners. In an array of resonators, these strips then link together, forming a bus for applying an external dc bias. All the varactors are therefore connected in parallel. Since each varactor is operated in reverse bias and draws current in the level of picoamps, the bias strips can be very thin and narrow despite a large number of resonators in the array. Owing to the electrically small size of these strips, together with their orthogonal alignment to the E-field polarization, their interaction with the electric field is minimal.

III. Fabrication

An array of the resonators as shown in Fig. 1(b) has been fabricated on an epoxy FR4 substrate with a thickness of 0.8 mm, a measured dielectric constant of 4.5, and a reported loss tangent of 0.02. The metal used for the resonators is bare copper with a thickness of 35 μm. The dimensions of each resonator are as follows: $a = 13$ mm, $d = 11$ mm, $l = 1.8$ mm, $w = 1.7$ mm, $b = 0.8$ mm, $g = 0.4$ mm, and $s = 0.3$ mm. These parameters result in an LC resonance in the microwave S-band. The entire array contains 20×20 resonators, which is large enough to span across the main beam of a nearby feeding horn antenna. The total board dimensions are 280×320 mm^2, including the dc bias area. The fabricated active resonator array is shown in Fig. 2. As a reference, a passive array with the same resonator shape, size, and number has also been fabricated, except that this array has no loaded varactor ($w = 0$ mm) and no dc bias strips.

Infineon BB837 surface-mounted diodes are used as varactors for resonance tuning. Their capacitance tolerance is within 5%. The relation between the junction capacitance $C_{\rm j}$ and the bias voltage $V_{\rm j}$ is given by [20]

$$C_{\rm j} = \frac{C_{\rm j0}}{(1 - V_{\rm j}/\psi_0)^m} + C_1. \tag{1}$$

The SPICE model yields the zero-bias junction capacitance $C_{\rm j0} = 9.122$ pF, the junction potential $\psi_0 = 6.223$ V, the junction grading coefficient $m = 2.42$, and the extra parallel capacitance $C_1 = 0.27$ pF. In addition to the junction capacitance, a package capacitance $C_{\rm ac} = 110$ fF (SOD323 package) also influences the LC resonance and will be considered in the simulation. Therefore, the total varactor capacitance $C_{\rm d}$ equals

$$C_{\rm d} = C_{\rm j} + C_{\rm ac}. \tag{2}$$

As these varactors are always operated in the reverse bias, the maximum current drawn by each varactor is only 25 pA at 28 V. In total, the active array drains a maximum current of only 10 nA in the steady state.

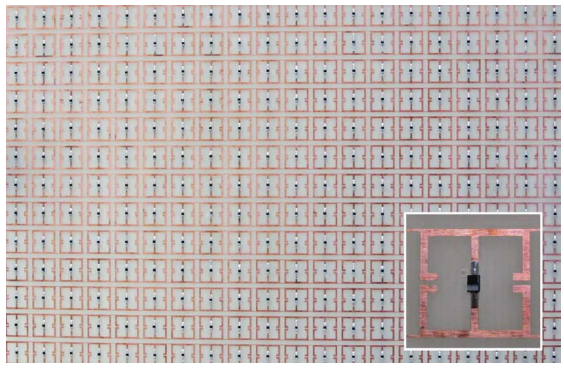

Fig. 2. Partial view of varactor-loaded ELC resonator array. *(inset)* Zoom-in for single resonator, with the varactor clearly visible in its center.

IV. Experiment and Discussion

A. Passive ELC Resonators

The measurement is carried out in an anechoic chamber with a pair of microwave horn antennas as transmitting and receiving ports, separated by 5 m. The receiving antenna is an ETS-Lindgren quadridge horn 3164-05 with an aperture size of 171×171 mm^2 and a 3-dB beamwidth of 22.5° (E-plane) and 35° (H-plane). Owing to its finite dimensions, the array needs to be placed close to the receiving antenna, i.e., 150 mm from the horn aperture, to cover the receiving beamwidth. The sample transmission is measured and compared to the free-space transmission. The experimental configuration is not ideal because of the plane-wave approximation and the finite size of the array in the lateral directions.

The simulation with ideal conditions is performed using Ansoft HFSS. Periodic boundary conditions are utilized for the transverse boundaries to replicate an infinite planar array of resonators. Two ports facing the array allow determining its response to a plane wave incident normally. The ports are deembedded onto the sample's surfaces to cancel the phase change introduced by free space propagation.

The results for the passive array are shown in Fig. 3. An excellent agreement is found between the measurement and simulation. On resonance at 2.69 GHz, the field attenuation is over 25 dB. Slightly off resonance, the transmission magnitude from the measurement is higher than that obtained from the simulation and even higher than 0 dB at high frequencies. This effect is attributed to alteration of the microwave beam pattern by the presence of the finite array, resulting in additional energy diffracted into the receiving horn. From the surface current distribution, it can be deduced that the observed resonance is based on an LC interaction because of the circulating current in the

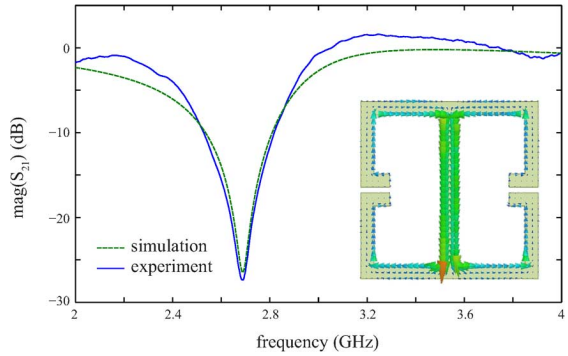

Fig. 3. Transmission magnitude for the passive resonator array. The resonance takes place at 2.69 GHz. The inset shows the on-resonance instantaneous surface current distribution over a unit cell obtained from the simulation.

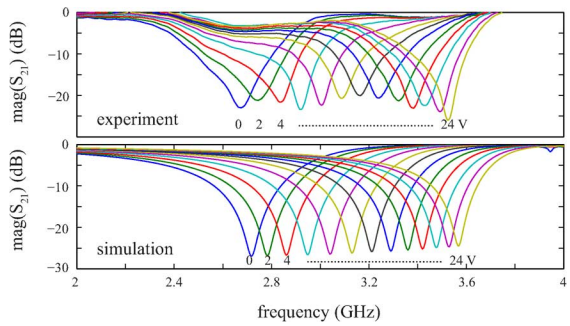

Fig. 4. Transmission magnitude for the active resonator array. The reverse bias applied to the varactors varies from 0 to 24 V with a step-size of 2 V.

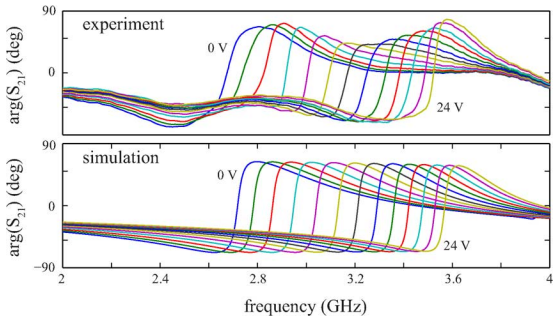

Fig. 5. Transmission phase for the active resonator array. The phase profiles correspond to the magnitude profiles in Fig. 4.

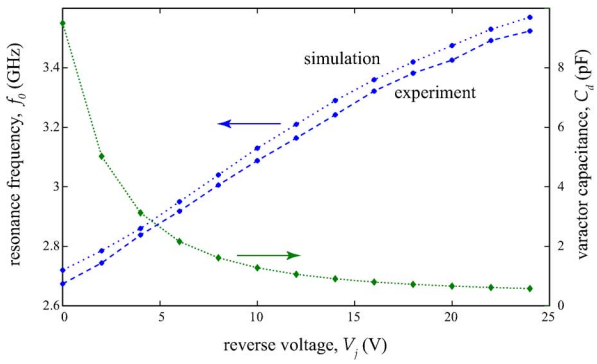

Fig. 6. Resonance frequency and varactor capacitance against reverse bias voltage. The capacitance is calculated from (2). The connecting lines are merely for visual guidance.

loops. The distribution further illustrates the current maximum in the middle of the central strip, the chosen site for the varactor.

B. Active ELC Resonators

The experimental configuration for the varactor-loaded array is similar to that for the passive array, except for the dc bias that is now incorporated to control the capacitance of the varactors. Owing to the free-space propagation and the low power of the microwave beam (0 dBm from the network analyzer), the nonlinear response of the resonators [19] can be neglected. In the corresponding simulation, a lumped capacitor is included in the unit cell, and its value is determined from the total varactor capacitance according to (2). The measured and simulated transmission characteristics for the active array at different dc biases are illustrated in Figs. 4 and 5.

The results from the simulation and experiment are in general agreement both in the magnitude and phase. The resonance frequency shows a strong dependence on the bias voltage, while the resonance shape is reasonably preserved. As the reverse bias increases from 0 to 24 V, the capacitance decreases, and the resonance experiences a shift from 2.67 to 3.52 GHz. Hence, the tunable range is nearly 32% with reference to the lower frequency, and it can be further increased as the maximum rating for the varactor reverse-bias voltage is in fact 30 V. The fluctuation in the resonance strength in the experimental results is ascribed to standing waves existing between the array and the horn antennas.

Fig. 6 plots the resonance frequency and the varactor capacitance as a function of the reverse-bias voltage. It illustrates a small and constant difference in the resonance frequency obtained from the simulation and the experiment. This systematic discrepancy is most likely due to the limited accuracy in the simulation and the parasitic inductance in the real varactors. Also observable in Fig. 6 is a nearly linear relationship between the resonance frequency and the bias voltage, despite a quadratic decrement in the varactor capacitance. This linear relationship results from compensation of the quadratic decrement by the resonance condition $\omega_0 = 1/\sqrt{LC}$.

C. Sensitivity Analysis

It is clear from the experimental results that the resonance frequency of the active resonator array is very sensitive to a change in the varactor capacitance. This results from optimal varactor placement. However, such a level of sensitivity might raise a question about the functionality for a large array containing hundreds or even thousands of varactors, whose capacitance values are not exactly identical. This situation could lead to inhomogeneous resonance broadening owing to a difference in the resonance frequencies among the resonators [15], [21], [22]. In response to this concern, a sensitivity analysis, based on the equivalent circuit of the resonator, is conducted to assess the tolerance of the array against a variation in the varactor capacitance. The circuit representing an ELC resonator, shown in the inset of Fig. 7, comprises two capacitors, C_s and C_d, and an inductor L_s, all connected in series, yielding the resonant frequency of

$$f_0 = \frac{1}{2\pi}\sqrt{\frac{C_\mathrm{s}+C_\mathrm{d}}{L_\mathrm{s}C_\mathrm{s}C_\mathrm{d}}}. \tag{3}$$

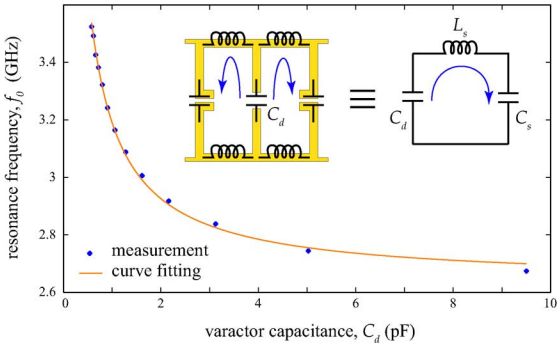

Fig. 7. Measured resonance frequency against varactor capacitance. The fitted curve is based on (3) with $C_{\rm s} = 0.46$ pF and $L_{\rm s} = 7.86$ nH. The inset shows the equivalent series LC circuit of the resonator. The arrows show the direction of the instantaneous current.

Here, $C_{\rm s}$ and $L_{\rm s}$ denote the capacitance and inductance of the unloaded resonator, including mutual interaction with neighbor elements, and $C_{\rm d}$ denotes the varactor capacitance. The two constant parameters, $C_{\rm s}$ and $L_{\rm s}$, specific to the ELC resonator, can be determined from curve fitting to the experimental relation between f_0 and $C_{\rm d}$, as indicated in Fig. 7.

From (3), the sensitivity of the resonance frequency to the varactor capacitance can be derived as

$$S_{C_{\rm d}}^{f_0} = \frac{C_{\rm d}}{f_0}\frac{\partial f_0}{\partial C_{\rm d}} = -\frac{C_{\rm s}}{2(C_{\rm s}+C_{\rm d})}. \tag{4}$$

Surprisingly, the sensitivity is not dependent on the inductance of the resonator. The manufacturer specifies a 5% worst-case variation in the varactor capacitance. Therefore, from (4), a variation in the resonance frequency owing to varactor mismatch will not exceed 1.1% at $V_{\rm j} = 24$ V ($C_{\rm d} = 0.58$ pF and $f_0 = 3.52$ GHz) and 0.1% at $V_{\rm j} = 0$ V ($C_{\rm d} = 9.5$ pF and $f_0 = 2.67$ GHz). This level of variation is considered insignificant for most applications.

V. Conclusion

This letter presents a large array of wideband-tunable microwave ELC resonators. Each resonator is loaded with a varactor at the location where the microwave-induced voltage gradient is maximal. As a result, the resonance frequency of the array can be electrically tuned from 2.67 to 3.52 GHz, equivalent to a tuning range of nearly 32%. No significant resonance distortion is observed across the tuning range. The sensitivity analysis further confirms the robustness of the resonator array against manufacturing tolerance in the capacitance values of the varactors.

In addition to its application as a building block for metamaterials, this tunable ELC resonator can effectively function as a component for active microwave devices, such as spatial filters or modulators. The proposed array has many benefits compared to a traditional frequency selective surface. Due to the inherently subwavelength dimensions of the resonator, the array can provide harmonic-free and angle-independent responses and steep phase gradient within a certain bandwidth. The angle independency allows positioning of the source or detector closer to the array [23], while the steep phase gradient results in greater steering capability for a reflectarray [16], for example.

Acknowledgment

The authors acknowledge I. Linke, B. Pullen, P. Simcik, and H. Ho for their technical assistance.

References

[1] D. Schurig, J. J. Mock, and D. R. Smith, "Electric-field-coupled resonators for negative permittivity metamaterials," *Appl. Phys. Lett.*, vol. 88, no. 4, p. 041109, 2006.
[2] W. J. Padilla, M. T. Aronsson, C. Highstrete, M. Lee, A. J. Taylor, and R. D. Averitt, "Electrically resonant terahertz metamaterials: Theoretical and experimental investigations," *Phys. Rev. B*, vol. 75, no. 4, p. 041102, 2007.
[3] S. Sajuyigbe, B. J. Justice, A. F. Starr, and D. R. Smith, "Design and analysis of three-dimensionalized ELC metamaterial unit cell," *IEEE Antennas Wireless Propag. Lett.*, vol. 8, pp. 1268–1271, 2009.
[4] H. Tao, N. I. Landy, C. M. Bingham, X. Zhang, R. D. Averitt, and W. J. Padilla, "A metamaterial absorber for the terahertz regime: Design, fabrication and characterization," *Opt. Exp.*, vol. 16, no. 10, pp. 7181–7188, 2008.
[5] Q. Cheng, T. J. Cui, W. X. Jiang, and B. G. Cai, "An omnidirectional electromagnetic absorber made of metamaterials," *New J. Phys.*, vol. 12, p. 063006, 2010.
[6] B. Zhu, Y. Feng, J. Zhao, C. Huang, and T. Jiang, "Switchable metamaterial reflector/absorber for different polarized electromagnetic waves," *Appl. Phys. Lett.*, vol. 97, p. 051906, 2010.
[7] H.-T. Chen, W. J. Padilla, M. J. Cich, A. K. Azad, R. D. Averitt, and A. J. Taylor, "A metamaterial solid-state terahertz phase modulator," *Nature Photon.*, vol. 3, pp. 148–151, 2009.
[8] J. Y. Chin, M. Lu, and T. J. Cui, "Metamaterial polarizers by electric-field-coupled resonators," *Appl. Phys. Lett.*, vol. 93, p. 251903, 2008.
[9] B. Zhu, Y. Feng, J. Zhao, C. Huang, Z. Wang, and T. Jiang, "Polarization modulation by tunable electromagnetic metamaterial reflector/absorber," *Opt. Exp.*, vol. 18, no. 22, pp. 23 196–23 203, 2010.
[10] A. C. Strikwerda, K. Fan, H. Tao, D. V. Pilon, X. Zhang, and R. D. Averitt, "Comparison of birefringent electric split-ring resonator and meanderline structures as quarter-wave plates at terahertz frequencies," *Opt. Exp.*, vol. 17, no. 1, pp. 136–149, 2009.
[11] L. Kang, Q. Zhao, H. Zhao, and J. Zhou, "Magnetic tuning of electrically resonant metamaterial with inclusion of ferrite," *Appl. Phys. Lett.*, vol. 93, p. 171909, 2008.
[12] H.-T. Chen, J. F. O'Hara, A. K. Azad, A. J. Taylor, R. D. Averitt, D. B. Shrekenhamer, and W. J. Padilla, "Experimental demonstration of frequency-agile terahertz metamaterials," *Nature Photon.*, vol. 2, pp. 295–298, 2008.
[13] N.-H. Shen, M. Massaouti, M. Gokkavas, J.-M. Manceau, E. Ozbay, M. Kafesaki, T. Koschny, S. Tzortzakis, and C. M. Soukoulis, "Optically implemented broadband blueshift switch in the terahertz regime," *Phys. Rev. Lett.*, vol. 106, p. 037403, 2011.
[14] B. Ozbey and O. Aktas, "Continuously tunable terahertz metamaterial employing magnetically actuated cantilevers," *Opt. Exp.*, vol. 19, no. 7, pp. 5741–5752, 2011.
[15] T. H. Hand and S. A. Cummer, "Controllable magnetic metamaterial using digitally addressable split-ring resonators," *IEEE Antennas Wireless Propag. Lett.*, vol. 8, pp. 262–265, 2009.
[16] T. H. Hand and S. A. Cummer, "Reconfigurable reflectarray using addressable metamaterials," *IEEE Antennas Wireless Propag. Lett.*, vol. 9, pp. 70–74, 2010.
[17] W. Withayachumnankul, C. Fumeaux, and D. Abbott, "Compact electric-LC resonators for metamaterials," *Opt. Exp.*, vol. 18, no. 25, pp. 25 912–25 921, 2010.
[18] I. V. Shadrivov, S. K. Morrison, and Y. S. Kivshar, "Tunable split-ring resonators for nonlinear negative-index metamaterials," *Opt. Exp.*, vol. 14, no. 20, pp. 9344–9349, 2006.
[19] D. A. Powell, I. V. Shadrivov, and Y. S. Kivshar, "Nonlinear electric metamaterials," *Appl. Phys. Lett.*, vol. 95, no. 8, p. 084102, 2009.
[20] T. H. Lee, *Planar Microwave Engineering*, 1st ed. Cambridge, U.K.: Cambridge Univ. Press, 2004.
[21] M. V. Gorkunov, S. A. Gredeskul, I. V. Shadrivov, and Y. S. Kivshar, "Effect of microscopic disorder on magnetic properties of metamaterials," *Phys. Rev. E*, vol. 73, no. 5, p. 056605, 2006.
[22] J. Gollub, T. Hand, S. Sajuyigbe, S. Mendonca, S. Cummer, and D. R. Smith, "Characterizing the effects of disorder in metamaterial structures," *Appl. Phys. Lett.*, vol. 91, no. 16, p. 162907, 2007.
[23] F. Bayatpur and K. Sarabandi, "Miniaturized FSS and patch antenna array coupling for angle-independent, high-order spatial filtering," *IEEE Antennas Wireless Propag. Lett.*, vol. 9, pp. 79–81, 2010.